

# Middle Miocene high-pressure metamorphism and fast exhumation of the Nevado-Filábride Complex, SE Spain

V. López Sánchez-Vizcaíno,<sup>1\*</sup> D. Rubatto,<sup>2</sup> M. T. Gómez-Pugnaire,<sup>3</sup> V. Trommsdorff<sup>4</sup> and O. Müntener<sup>5</sup>

<sup>1</sup>Departamento de Geología, Universidad de Jaén, E.U. Politécnica de Linares, C/Alfonso X el Sabio, 28, 23700 Linares, Spain; <sup>2</sup>The Australian National University, Research School of Earth Sciences, Mills Road, 0200 Canberra, Australia; <sup>3</sup>Departamento de Mineralogía y Petrología, Universidad de Granada, Campus Fuentenueva s/n, 18002 Granada, Spain; <sup>4</sup>Institute for Mineralogy and Petrography, ETH-Zurich, ETH-Zentrum, CH-8092 Zurich, Switzerland; <sup>5</sup>Geological Institute, University of Neuchâtel, CH-2007 Neuchâtel, Switzerland

## ABSTRACT

This study provides new constraints on fast cooling and exhumation rates of high-pressure metamorphic rocks in young active mountain belts. Ion microprobe (SHRIMP) U–Pb analysis of zircon in a pyroxenite layer of the Cerro del Almiraz ultramafic rocks (Nevado-Filábride Complex, southern Spain) gave an age of  $15.0 \pm 0.6$  Myr (95% c.l.). Mineral inclusions demonstrate that zircon formed close to the high-pressure peak. Combined with previous fission track data, the 15 Myr age suggests high cooling ( $\sim 80$  °C Myr<sup>-1</sup>) and exhumation ( $\sim 1.2$  cm yr<sup>-1</sup>) rates

for the unit. The new results indicate that both the Nevado-Filábride Complex and the overlying Alpujárride Complex, with somewhat higher ages and exhumation rates, underwent similar metamorphic evolutions at different times. This implies that the Alpujárride rocks were exhumed when the Nevado-Filábride was subducting and that the same tectonic scenario propagated from one portion of the Betic Cordilleras to another.

Terra Nova, 13, 327–332, 2001

## Introduction

The Betic Cordilleras, southern Spain, and the Rif Mountains of Morocco (Fig. 1) are one of the youngest and more active portions of the Alpine orogen and are thus particularly suitable for the study of fast tectonic processes. They formed during convergence between the African and Iberian plates in the Tertiary period (Dewey *et al.*, 1989) and underwent large-scale extensional collapse in the early Miocene (Galindo-Zaldívar *et al.*, 1989; Platt and Vissers, 1989). Extension was accommodated by thin-skinned fold belts at the periphery of the system and coeval subsidence to form the Alborán marine basin.

The Nevado-Filábride Complex (NFC) and the overlying Alpujárride Complex (AC) are part of the Internal Zones of the Betic Cordilleras and record Alpine high pressure (HP) metamorphism (Gómez-Pugnaire and Fernández-Soler, 1987; Goffé *et al.*, 1989; Tubía and Gil-Ibarguchi, 1991). During exhumation, the HP rocks were partially overprinted by amphibolite and greenschist facies retrograde

assemblages. Extremely high exhumation ( $3$  cm yr<sup>-1</sup>) and cooling rates ( $200$ – $340$  °C Myr<sup>-1</sup>) have been proposed for the AC (Sánchez-Rodríguez and Gebauer, 2000), but they do not seem to apply to the early evolution of the NFC, despite evidence for fast tectonic denudation in the late history of this latter unit. This *apparent* inconsistency is the consequence of the scattered radiometric dating of metamorphism in the NFC from mid-Cretaceous (Andriessen *et al.*, 1991) through Eocene to Miocene (Monié *et al.*, 1991; De Jong *et al.*, 1992; Zeck *et al.*, 1992; Puga *et al.*, 1996; Nieto *et al.*, 1997), and the lack of real age constraints for the high-pressure event.

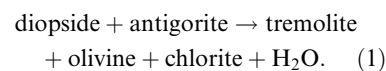
The present contribution uses new U–Pb data for zircons from a pyroxenite within ultramafic rocks of the NFC to constrain the age of HP metamorphism. These data are then combined with published fission track ages in order to draw a new pressure–temperature–time (P–T–t) path for this complex. This is a crucial step for calculating cooling and exhumation rates for the NFC and for testing the hypothesis of fast exhumation in this section of the Alpine belt.

## Ultramafic rocks of Sierra Nevada

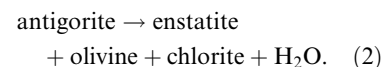
Ultramafic rocks are found throughout the upper sequence of the NFC

(Fig. 1) forming strongly deformed sheets or lenses. The largest of these bodies ( $400$  m  $\times$   $2$  km) occurs in the Sierra Nevada at Cerro del Almiraz. The ultramafic rocks often display a compositional layering with clinopyroxene-poor and clinopyroxene-rich layers. They also contain variably rodingitized mafic and pyroxenitic dykes, and dunitic pods (Morten and Puga, 1984; Trommsdorff *et al.*, 1998; Hürlimann, 1999; Puga *et al.*, 1999; Schönbächler, 1999).

At Cerro del Almiraz, the upper part of the ultramafic sheet is made of foliated serpentinite which consists of magnetite + diopside ( $\pm$  tremolite) + chlorite + antigorite  $\pm$  titanian clinohumite. This assemblage formed according to the reaction (Fig. 2)



The lower part of the thrust sheet is dominated by a more massive rock with tremolite + chlorite + enstatite + forsterite  $\pm$  titanian clinohumite, which formed according to (Fig. 2)



The contact between the two ultramafic rock types is irregular and is interpreted as the isograd defined by reaction (2) with no tectonic discontinuity (Schönbächler, 1999).

\*Correspondence: V. López Sánchez-Vizcaíno, Departamento de Geología, Universidad de Jaén, E.U. Politécnica de Linares, C/Alfonso X el Sabio, 28, 23700 Linares, Spain. Tel.: +34 953026523; fax: +34 953026508; e-mail: vlopez@ujaen.es

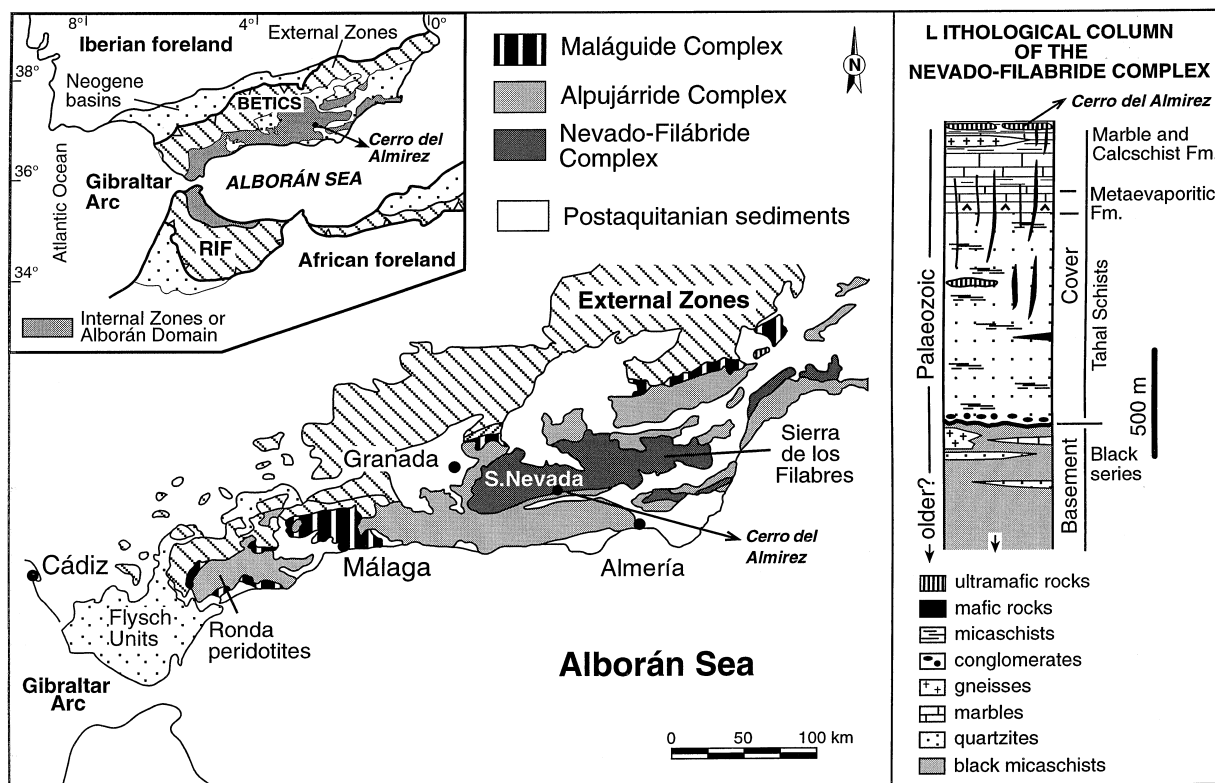
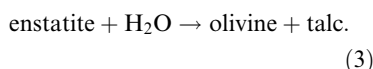


**Fig. 1** Geological map of the Internal Zones of the Betic Cordilleras, with Cerro del Almirez details, and lithological column of the Nevado-Filábride Complex showing the position of the dated ultramafic rocks.

During retrogression, enstatite was partially replaced by talc according to the reaction



Reactions (1)–(3) and their two intersections bracket the maximum *P* and *T* around 2 GPa and 700 °C for the ultramafic thrust sheet. The data also allow a retrograde *P*–*T* path to be constructed (Fig. 2) which is consistent with that for the surrounding metapelites (Schönbächler, 1999).

### Sample description and geochronology

#### Petrography

The dated zircon was obtained from a meta-clinopyroxenite boudin within serpentinites just outside the isograd across which enstatite plus olivine formed. The diopsidic clinopyroxene ( $X_{\text{Mg}} = 0.91\text{--}0.93$ ) is dusted with inclusions of Cr-bearing magnetite

and ilmenite lamellae. New, clear clinopyroxene ( $X_{\text{Mg}} = 0.95\text{--}0.98$ ) overgrew the inclusion-rich generation along grain margins. The recrystallized matrix minerals comprise olivine, diopside, antigorite, minor tremolite, chromian magnetite and titanian clinohumite. Zircon and tiny zirconolite grains are found in small domains near titanian clinohumite or together with its breakdown products.

The investigated pyroxenite contains two different zircon populations. The majority of the zircon grains are small ( $\leq 100 \mu\text{m}$ ), opaque and locally preserve crystal faces. In cathodoluminescence, these grains have homogeneous emission and do not show any regular zoning pattern (Fig. 3a). They contain inclusions of diopside, Al-rich antigorite and chlorite. A few zircon crystals are clear, pink and preserve crystal faces with rounded edges. This second population displays oscillatory zoning truncated by the outer shape (Fig. 3b) suggesting that the crystals were broken, corroded or abraded, possibly

before being incorporated into the ultramafic rock.

#### Analytical methods

Zircons were separated according to magnetic properties and density and finally selected by hand-picking. After being embedded in epoxy, cathodoluminescence images were taken with a Hitachi S2250N Scanning Electron Microscope. Zircon domains free of inclusions were analysed for U, Th and Pb using the SHRIMP II ion microprobe at the Research School of Earth Sciences, Australian National University. Instrumental conditions and data acquisition were as described by Compston *et al.* (1992) using zircon from the Duluth gabbro (AS3) and from Sri Lanka (SL13) as standards. The data were corrected for common lead via the measured  $^{207}\text{Pb}/^{206}\text{Pb}$  ratio. In the absence of any evidence for intrinsic common Pb in the zircons, Broken Hill common lead composition, which approximates the laboratory background common Pb, has been used.

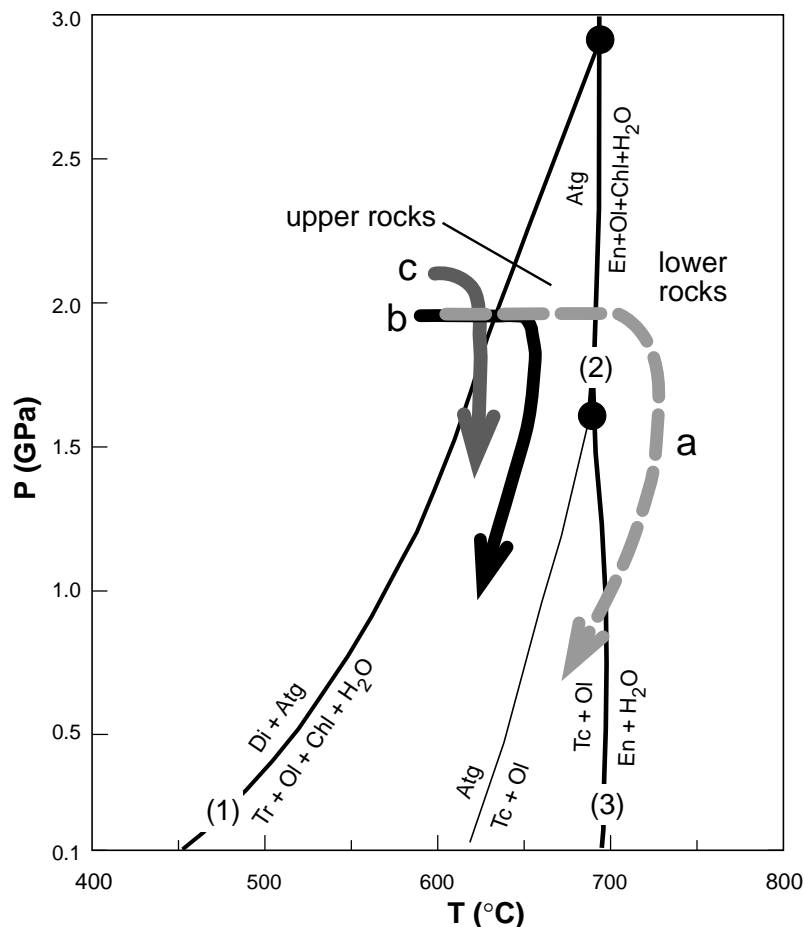


**Fig. 2** P–T evolution deduced for the ultramafic rocks of the Cerro del Almirez outcrop (path a), for the dated meta-clinopyroxenite (path b), and for the surrounding metapelites (path c) (Schönbächler, 1999). Upper and lower rocks refer to the position within the Almirez ultramafic sheet. The rocks in the upper part are foliated serpentinites (antigorite + olivine + diopside ± tremolite + chlorite), whereas in the lower part rocks are more massive consisting of enstatite + olivine + tremolite + chlorite. Location of reaction (1) (see text for details) has been calculated using Vertex (Connolly, 1990) and the Berman (1988) database and taking into account the observed substitution of Fe for Mg in the following minerals ( $X_{Mg}$  for Ol = 0.89; Atg = 0.95; Di = 0.96; Tr = 0.95; where  $X_{Mg} = Mg/(Mg + Fe)$ ). Location of reactions (2) and (3) (see text for details) has been taken from experimental determinations reported by Ulmer and Trommsdorff (1999). Reaction Atg → Tlc + Ol (thin line) brackets the stability field of Tlc. Many other reactions have been omitted for clarity.

### SHRIMP U–Pb ages

The unzoned zircons have relatively homogeneous and low U- and Th-contents (Table 1). Eleven of the 12 SHRIMP analyses on nine different grains yield ages between 19.0 and 14.1 Myr which average at  $15.0 \pm 0.6$  Myr (95% c.l., Fig. 4). One analysis excluded from the calculation – which yields a significantly older age – was partially measured on a large inclusion of antigorite. The three

pink and clear zircons are characterized by variable U and Th concentrations and yield concordant ages around 450 and 560 Myr (Fig. 4).

### Time of zircon growth

The presence of metamorphic mineral inclusions demonstrates that the zircons grew during HP metamorphism. This conclusion is supported by the absence of planar crystal faces and oscillatory zoning in the zircon, which

would instead support a magmatic origin. The inclusions found in the 15-Myr-old zircon represent the mineral assemblage stable prior to or at the HP breakdown of antigorite (Fig. 2). It is suggested that the relatively high temperature (> 630 °C) at the metamorphic peak and the concomitant fluid release are likely to have triggered the formation of the zircons at 15 Myr. Fluid production was triggered by the incipient breakdown of antigorite + diopside [see eqn (1) and Fig. 2], which closely precedes the final breakdown of antigorite [see eqn (2) and Fig. 2] (Trommsdorff *et al.*, 1998). Therefore, the 15 Myr age is interpreted herein as dating the thermal peak at pressures of ~2.0 GPa.

The two zircons dated at around 450–465 Myr have oscillatory zoning typical of magmatic zircon and show evidence of corrosion and abrasion. The 562-Myr-old crystal contains inclusions of quartz and biotite indicating that this grain represents a xenocryst that did not form in the mantle but rather in the crust. It is likely that these Palaeozoic zircon crystals derived from crustal material recycled into the mantle that were then incorporated into the pyroxenite during its formation.

## Discussion

### The age of Alpine HP metamorphism

The inclusions, morphology and textural relationships of the 15-Myr-old zircon grains indicate that they grew at the thermal peak of metamorphism. In the ultramafic rocks, the thermal peak was reached near the HP conditions (Trommsdorff *et al.*, 1998) and was followed by cooling and decompression (Puga *et al.*, 1999). The new U–Pb data presented herein suggest a much younger age than previously proposed for the HP event in the NFC.

The previous Palaeogene to Cretaceous age estimates were inferred from dating of the cooling path (Andriessen *et al.*, 1991; Monié *et al.*, 1991; De Jong *et al.*, 1992; Zeck *et al.*, 1992; Puga *et al.*, 1996). An effort to measure Sm–Nd on eclogites from the Mulhacén Complex documented isotopic disequilibrium (Nieto *et al.*, 1997). Similar problems have been

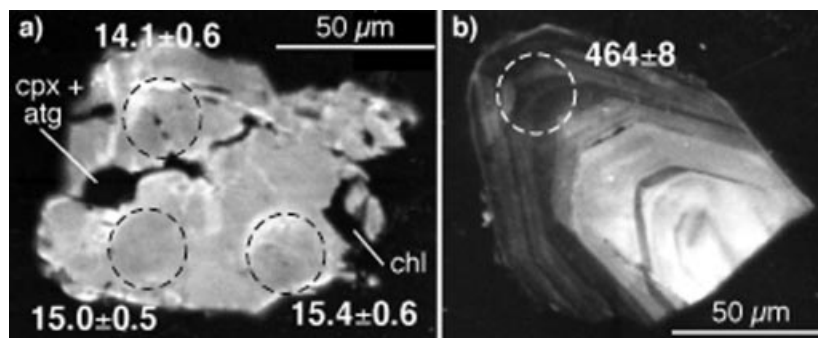


**Fig. 3** Cathodoluminescence image of (a) an Alpine zircon with no regular pattern and (b) an Ordovician zircon grain with magmatic zoning.

encountered using the K–Ar and Rb–Sr systems, which yielded anomalously old and erratic ages attributed to incomplete degassing and excess argon (67 and 43 Myr, Puga *et al.*, 1996; 836–14 Myr, Andriessen *et al.*, 1991), or repeated resetting by volcanic fluids (30–14 Myr, De Jong *et al.*, 1992). Monié *et al.* (1991) suggested an Eocene age for metamorphism and slow exhumation of the Sierra de los Filabres on the basis of dubious  $^{40}\text{Ar}$ – $^{39}\text{Ar}$  data but their interpretation contrasts with several later publications that documented fast cooling and exhumation in the Betic Cordillera (Zeck *et al.*, 1992; Monié *et al.*, 1994; Johnson *et al.*, 1997; Platt and Whitehouse, 1999; Sánchez-Rodríguez and Gebauer, 2000).

### Exhumation history

The best constraints on the late metamorphic evolution of the NFC origin-

ate from zircon fission track data, which have been interpreted as cooling to  $230 \pm 25$  °C between 12 and 9 Myr (Johnson *et al.*, 1997). These authors estimated, using apatite modelling, that cooling was more or less complete by 11 Myr in the east and 8 Myr in the west. Thus, it could be assumed that the Cerro del Almiraz rocks, which are located in an intermediate position, cooled below  $\sim 230$  °C by  $\sim 10$  Myr. The fission track data are in agreement with sedimentological data. The first influx of clastic sediments shed from the NFC in the adjacent basins took place during the Serravallian ( $\sim 11$  Myr) in the east (Braga and Martín, 1988) and during the late Tortonian (less than 8.5 Myr) in the west (Rodríguez Fernández, 1983).

The rates of exhumation and cooling of the studied NF rocks can be estimated combining the fission-track and sedimentological data with the new

SHRIMP age (Fig. 5). It is assumed that exhumation begun at 15 Myr, shortly after peak metamorphism (minimum conditions of 18 GPa = 67 km and  $\sim 630$  °C). At around 10 Myr and 230 °C (blocking temperature for zircon fission tracks according to Johnson *et al.*, 1997), the NFC rocks reached a depth ranging between  $\sim 7$  and 10 km (0.2–0.3 GPa) depending on the assumed geotherm (Spear, 1993). These results point to a fast exhumation at a rate of  $\sim 1.1$ – $1.2$  cm  $\text{yr}^{-1}$ , which is comparable, even though slightly slower, to those estimated for other eclogitic terrains within the Alpine chain (Gebauer *et al.*, 1997; Sánchez-Rodríguez and Gebauer, 2000; Rubatto and Hermann, 2001).

The resulting minimum cooling rate is  $\sim 80$  °C  $\text{Myr}^{-1}$ , which is lower than that calculated by Johnson *et al.* (1997) for the late cooling of the NFC (ranging from 105 °C to 170 °C  $\text{Myr}^{-1}$ ). However, the lower cooling rate deduced for the Cerro del Almiraz is still in line with the thermal evolution expected for deep rocks being exhumed at very fast rates. It is to be expected that cooling rates were relatively slow at depth and dramatically increased at shallower levels with decreasing exhumation rates (Johnson *et al.*, 1997).

### Tectonic implications

The temperature–time paths shown in Fig. 5 indicate that the NFC underwent a similar thermal evolution to the overlying AC (Zeck and White-

**Table 1** U–Th–Pb SHRIMP analyses on zircons from the Almiraz pyroxenite. Errors are at  $1\sigma$  levels

Label	U (ppm)	Th (ppm)	Th/U	% com Pb	$^{238}\text{U}/^{206}\text{Pb}^*$	$^{207}\text{Pb}/^{206}\text{Pb}^*$	$^{206}\text{Pb}/^{238}\text{U}^\dagger$	Age $^\ddagger$ $^{206}\text{Pb}/^{238}\text{U}$
AL-5.1	37.7	40.6	1.08	21.46	322.54 $\pm$ 9.43	0.2428 $\pm$ 151	0.00244 $\pm$ 9	15.68 $\pm$ 0.56
AL-5.2	20.1	16.8	0.84	25.89	271.09 $\pm$ 17.59	0.2834 $\pm$ 235	0.00273 $\pm$ 20	17.60 $\pm$ 1.29
AL-6.1	16.8	1.8	0.11	52.25	162.22 $\pm$ 5.16	0.5247 $\pm$ 410	0.00294 $\pm$ 29	18.95 $\pm$ 1.88
AL-7.1	123.4	91.8	0.74	15.97	350.94 $\pm$ 12.43	0.1926 $\pm$ 69	0.00239 $\pm$ 9	15.42 $\pm$ 0.56
AL-7.2	76.3	55.1	0.72	9.9	386.44 $\pm$ 10.20	0.1369 $\pm$ 159	0.00233 $\pm$ 8	15.01 $\pm$ 0.49
AL-7.3	70.3	55.6	0.79	15.52	385.01 $\pm$ 14.86	0.1884 $\pm$ 119	0.00219 $\pm$ 9	14.13 $\pm$ 0.59
AL-8.1	127.3	72.1	0.57	25.07	307.47 $\pm$ 16.18	0.2759 $\pm$ 403	0.00244 $\pm$ 19	15.69 $\pm$ 1.24
AL-9.1	228.5	191.0	0.84	7.07	425.16 $\pm$ 12.68	0.1110 $\pm$ 66	0.00219 $\pm$ 7	14.08 $\pm$ 0.43
AL-9.2	39.5	32.1	0.81	24.68	331.14 $\pm$ 9.22	0.2723 $\pm$ 152	0.00227 $\pm$ 8	14.65 $\pm$ 0.52
AL-9.3	16.7	11.2	0.67	56.91	156.84 $\pm$ 5.19	0.5674 $\pm$ 291	0.00275 $\pm$ 22	17.69 $\pm$ 1.43
AL-9.4	125.2	96.1	0.77	6.97	391.65 $\pm$ 11.01	0.1102 $\pm$ 63	0.00238 $\pm$ 7	15.29 $\pm$ 0.44
AL-4.1 <sup>ex</sup>	25.1	3.5	0.14	58.05	112.59 $\pm$ 3.77	0.5778 $\pm$ 174	0.00373 $\pm$ 21	23.97 $\pm$ 1.35
AL-1.1 <sup>os</sup>	1426.9	80.2	0.06	0.05	13.39 $\pm$ 0.230	0.0568 $\pm$ 2	0.07465 $\pm$ 128	464 $\pm$ 8
AL-2.1 <sup>os</sup>	33.7	17.0	0.50	0.09	10.96 $\pm$ 0.180	0.0597 $\pm$ 12	0.09114 $\pm$ 150	562 $\pm$ 9
AL-3.1 <sup>os</sup>	379.4	15.6	0.04	0.15	13.79 $\pm$ 0.258	0.0574 $\pm$ 4	0.07238 $\pm$ 135	451 $\pm$ 8

<sup>os</sup>, oscillatory zoned; \*uncorrected for common Pb;  $^\dagger$ corrected for common Pb; <sup>ex</sup>, excluded from age calculation.

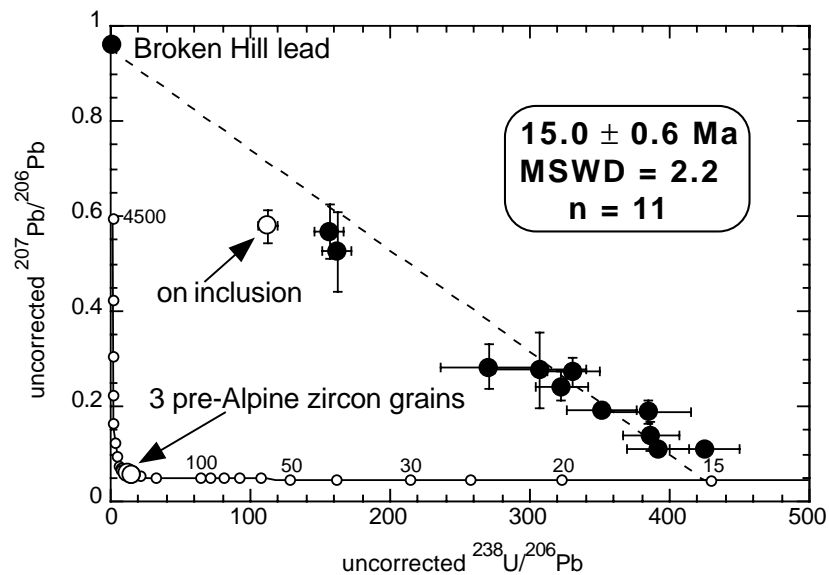


Fig. 4 Tera–Wasserburg plot for uncorrected data. Errors are plotted at the  $2\sigma$  level and the mean age is given at the 95% confidence level.

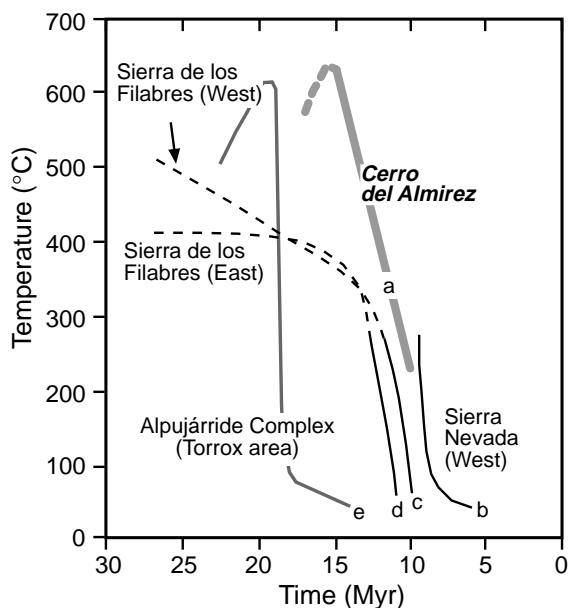


Fig. 5 Time–temperature plot showing: (a) the cooling curve calculated for the Cerro del Almiraz HP rocks; (b, c, d) the cooling curves of three transects for the uppermost structural levels within the NFC (Johnson *et al.*, 1997), including the curves (dashed lines) calculated by these authors for the radiometric data of De Jong (1991) and Monié *et al.* (1991); and (e) the cooling path calculated by Zeck and Whitehouse (1999) for the Alpujarride rocks of the Torrox area. Note (i) that the NFC and AC paths are subparallel if the new data reported here are considered and (ii) how they cross if previous radiometric data are considered.

house, 1999), but at different times (Fig. 5). In fact, geochronological (Platt and Whitehouse, 1999; Zeck and Whitehouse, 1999; Sánchez-Rod-

riguez and Gebauer, 2000) and sedimentological data (Braga *et al.*, 1996) indicate that the upper units of the AC underwent HP metamorphism before

or at 20 Myr and were already exhumed at 18–15 Myr. At this time (4–8 Myr before its exhumation) the NFC was still being subducted. This interpretation contrasts with previous models for the tectonic history of the two complexes. Such models were based on geochronological data (De Jong, 1991; Monié *et al.*, 1991) indicating that HP metamorphism in the NFC preceded that of the AC and implied a crossover in the time–depth paths of both units (Fig. 5).

A subsequent tectonic implication of the 15 Myr age for HP metamorphism in the NFC is that subduction in the Betic Chain lasted at least until the middle Miocene, longer than previously thought. In fact, active continental subduction has been recently detected below the Betic Cordillera and the Alborán Sea (Morales *et al.*, 1999). Furthermore, the fact that two units (NFC and AC) underwent *parallel but not synchronous* metamorphic histories is an important result: it implies that subduction and exhumation can act simultaneously within an orogen during the tectonic evolution of young collisional belts. In this case, the P–T evolution of the NFC and AC can be explained by exhumation mechanisms (see Lonergan and White, 1997 for discussion), that propagated through the Betic Chain during the Miocene.

#### Acknowledgements

This work was supported by Swiss National Foundation research grant no. 2000-050454.97/1 to V. Trommsdorff, and a postdoctoral fellowship to Daniela Rubatto. The Research School of Earth Sciences at ANU is thanked for support to Daniela Rubatto, and the Electron Microscope unit at the ANU for access to the SEM facilities. V. López Sánchez-Vizcaino and M.T. Gómez-Pugnaire are grateful to J.C. Braga and A. Azor for their comments and acknowledge support by DGICYT Projects PB95-1266 and BTE2000-1489, and RNM-0145 Group of the Junta de Andalucía. Reviews by D. Gebauer, A. Möller and B. Kober and comments from A. Kröner helped to improve the paper.

#### References

Andriessen, P.A.M., Hebeda, E.H., Simon, O.J. and Verschure, R.H., 1991. Tourmaline K–Ar ages compared to other

- radiometric dating systems in Alpine anatectic leucosomes and metamorphic rocks (Cyclades and southern Spain). *Chem. Geol.*, **91**, 33–48.
- Berman, R.G., 1988. Internally consistent thermodynamic data for minerals in the system  $\text{Na}_2\text{O} - \text{K}_2\text{O} - \text{CaO} - \text{MgO} - \text{FeO} - \text{Fe}_2\text{O}_3 - \text{SiO}_2 - \text{TiO}_2 - \text{H}_2\text{O} - \text{CO}_2$ . *J. Petrol.*, **29**, 445–522.
- Braga, J.C. and Martín, J.M., 1988. Neogene coralline-algal growth-forms and their palaeoenvironments in the Almazora river valley (Almería, S.E. Spain). *Palaeogeogr. Palaeoclim. Palaeoecol.*, **67**, 285–303.
- Braga, J.C., Jiménez, A.P., Martín, J.M. and Rivas, P., 1996. Middle Miocene coral-Oyster reefs, Murchas, Granada, Southern Spain. In: *Models for Carbonate Stratigraphy from Miocene Reef Complexes of Mediterranean Regions* (E.K. Franseen et al., eds), SEPM Concepts in Sedimentology and Paleontology 5, pp. 131–139. SEPM, Tulsa.
- Compston, W., Williams, I.S., Kirschvink, J.L., Zhang, Z. and Ma, G., 1992. Zircon U-Pb ages for the Early Cambrian timescale. *J. Geol. Soc. London*, **149**, 171–184.
- Connolly, J.A.D., 1990. Multivariable phase diagrams: an algorithm based on generalized thermodynamics. *Am. J. Sci.*, **290**, 666–718.
- De Jong, K., 1991. *Tectono-metamorphic studies and radiometric dating in the Betic Cordilleras (SE Spain)*. Doctoral dissertation, Vrije Universiteit Amsterdam, Elinkwijk, Utrecht.
- De Jong, K., Wijbrans, J.R. and Feraud, G., 1992. Repeated thermal resetting of phengites in the Mulhacén Complex (Betic Zone, southeastern Spain) shown by  $^{40}\text{Ar}/^{39}\text{Ar}$  step heating and single grains laser probe dating. *Earth. Planet. Sci. Lett.*, **110**, 173–191.
- Dewey, J.F., Helman, M.L., Turco, E., Hutton, D.H.W. and Knott, S.D., 1989. Kinematics of western Mediterranean. In: *Conference on Alpine Tectonics* (M.P. Coward et al., eds). *Spec. Publ. Geol. Soc. London*, **45**, 265–283.
- Galindo-Zaldívar, J., González-Lodeiro, F. and Jabaloy, A., 1989. Progressive extensional shear structures in a detachment contact in the Western Sierra Nevada (Betic Cordilleras, Spain). *Geodinam. Acta*, **3**, 73–85.
- Gebauer, D., Schertl, H.-P., Brix, M. and Schreyer, W., 1997. 35 Ma old ultrahigh-pressure metamorphism and evidence for very rapid exhumation in the Dora Maira Massif, Western Alps. *Lithos*, **41**, 5–24.
- Goffé, B., Michard, A., García-Dueñas, V. et al., 1989. First evidence of high-pressure, low-temperature metamorphism in the Alpujárride nappes, Betic Cordilleras (S.E. Spain). *Eur. J. Mineral.*, **1**, 139–142.
- Gómez-Pugnaire, M.T. and Fernández-Soler, J.M., 1987. High-pressure metamorphism in metabasites from the Betic Cordilleras (SE Spain) and its evolution during the Alpine orogeny. *Contr. Miner. Petrol.*, **95**, 231–244.
- Hürlimann, R., 1999. *Die Hochdruckmetamorphose der Ultramafika und der angrenzenden Nebengesteine am Cerro de Almirez, Sierra Nevada, Südsippanien (Teil II)*. Unpubl. Diplomarbeit, ETH, Zurich.
- Johnson, C., Harbury, N. and Hurford, A.J., 1997. The role of extension in the Miocene denudation of the Nevado-Filábride Complex, Betic Cordillera (SE Spain). *Tectonics*, **16**, 189–204.
- Lonergan, L. and White, N., 1997. Origin of the Betic-Rif mountain belt. *Tectonics*, **16**, 504–522.
- Monié, P., Galindo-Zaldívar, J., Goffé, B. and Jabaloy, A., 1991. First report on  $^{40}\text{Ar}/^{39}\text{Ar}$  geochronology of alpine tectonism in the Betic cordilleras (southern Spain). *J. Geol. Soc. London*, **148**, 289–297.
- Monié, P., Torres-Roldán, R.L. and García-Casco, A., 1994. Cooling and exhumation of the Western Betic Cordilleras,  $^{40}\text{Ar}/^{39}\text{Ar}$  thermochronological constraints on a collapsed terrane. *Tectonophysics*, **238**, 353–379.
- Morales, J., Serrano, I., Jabaloy, A. et al., 1999. Active continental subduction beneath the Betic Cordillera and the Alborán Sea. *Geology*, **27**, 735–738.
- Morten, L. and Puga, E., 1984. Blades of olivines and orthopyroxenes in ultramafic rocks from the Cerro del Almirez, Sierra Nevada Complex, Spain: relics of quench-textured harzburgites. *N. Jb. Miner. Mh.*, **5**, 211–218.
- Nieto, J.M., Puga, E., Monié, P.D., Díaz de Federico, A. and Jagoutz, E., 1997. High-pressure metamorphism in meta-granites and orthogneiss from the Mulhacén Complex (Betic Cordillera, Spain). *Terra Abstracts*, **9(1)**, 22–23.
- Platt, J.P. and Vissers, R.L.M., 1989. Extensional collapse of thickened continental lithosphere: a working hypothesis for the Alborán sea and Gibraltar arc. *Geology*, **17**, 540–543.
- Platt, J.P. and Whitehouse, M.J., 1999. Early Miocene high-temperature metamorphism and rapid exhumation in the Betic Cordillera (Spain): evidence from U-Pb zircon ages. *Earth Planet. Sci. Lett.*, **171**, 591–605.
- Puga, E., Nieto, J.M.D., Díaz de Federico, A., Bodinier, J.L. and Morten, L., 1999. Petrology and metamorphic evolution of ultramafic rocks and dolerite dykes of the Betic Ophiolitic Association (Mulhacén Complex, SE Spain): evidence of eo-Alpine subduction following an ocean-floor metasomatic process. *Lithos*, **49**, 23–56.
- Puga, E., Nieto, J.M.D., Díaz de Federico, A., Portugal, M. and Reyes, E., 1996. The intra-orogenic Sopontújar Formation of the Mulhacén Complex: Evidence of the polycyclic character of the Alpine orogeny in the Betic Cordilleras. *Eclog. geol. Helv.*, **89**, 129–162.
- Rodríguez Fernández, J., 1983. *El Mioceno del sector central de las Cordilleras Béticas*. Unpubl. doctoral dissertation, University of Granada.
- Rubatto, D. and Hermann, J., 2001. Exhumation as fast as subduction? *Geology*, **29**, 3–6.
- Sánchez-Rodríguez, L. and Gebauer, D., 2000. Mesozoic formation of pyroxenites and gabbros in the Ronda area (southern Spain), followed by Early Miocene subduction metamorphism and emplacement into the middle crust: U-Pb sensitive high-resolution ion microprobe dating of zircon. *Tectonophysics*, **316**, 19–44.
- Schönbächler, M., 1999. *Die Hochdruckmetamorphose der Ultramafika und der angrenzenden Nebengesteine am Cerro de Almirez, Sierra Nevada, Südsippanien (Teil I)*. Unpubl. Diplomarbeit, ETH, Zurich.
- Spear, F.S., 1993. Metamorphic phase equilibria and Pressure–Temperature–Time paths. *Mineralogical Society of America*, Washington.
- Trommsdorff, V., López Sánchez-Vizcaino, V., Gómez-Pugnaire, M.T. and Mün-tener, O., 1998. High pressure breakdown of antigorite to spinifex-textured olivine and orthopyroxene, SE Spain. *Contr. Miner. Petrol.*, **132**, 139–148.
- Tubía, J.M. and Gil-Ibarguchi, J.I., 1991. Eclogites of the Ojen nappe: a record of subduction in the Alpujárride Complex (Betic Cordilleras, southern Spain). *J. Geol. Soc. London*, **148**, 801–804.
- Ulmer, P. and Trommsdorff, V., 1999. Phase relations of hydrous mantle subducting to 300 km. In: *Mantle Petrology: Field Observations and High Pressure Experimentation* (Y. Fei et al., eds). *Spec. Publ. Geochem. Soc.*, **6**, 259–281.
- Zeck, H.P. and Whitehouse, M.J., 1999. Hercynian, Pan-African, Proterozoic and Archean ion-microprobe zircon ages for a Betic-Rif core complex, Alpine belt, W Mediterranean – consequences for its P-T-t path. *Contr. Miner. Petrol.*, **134**, 134–149.
- Zeck, H.P., Monié, P., Villa, I.M. and Hansen, B.T., 1992. Very high rates of cooling and uplift in the Alpine belt of the Betic Cordilleras, southern Spain. *Geology*, **20**, 79–82.

Received 13 March 2000; revised version accepted 17 July 2001